Cellulose (2023) 30:2667–2686
https://doi.org/10.1007/s10570-023-05042-w

ORIGINAL RESEARCH

Reduced graphene oxide/polyurethane coatings for wash-durable wearable piezoresistive sensors

Federico Olivieri · Gennaro Rollo · Francesca De Falco · Roberto Avolio · Irene Bonadies · Rachele Castaldo · Mariacristina Cocca · Maria Emanuela Errico · Marino Lavorgna · Gennaro Gentile

Received: 26 August 2022 / Accepted: 2 January 2023 / Published online: 11 January 2023

Abstract Graphene-based functional coatings for cotton textiles were realized through an easy dip-coating procedure. Cotton fabrics were coated with a reduced graphene oxide (rGO) layer and then protected with a very thin polyurethane (PU) layer that does not affect the flexibility and the hand of the pristine cotton. The application of the rGO coating induces electrical conductivity to the fabric and the application of the PU phase increases the durability of the coatings, that show very stable surface resistivity after 10 washing cycles performed at temperatures up to 40 °C. Furthermore, the rGO and rGO/PU coated fabrics show good comfort properties, increased thermal conductivity and breathability with respect to cotton. In particular, the realized coatings allow to confine the heat transfer in correspondence of a localized heating source, which is very interesting for thermal therapy applications. Finally, the rGO/PU coated fabrics present a piezoresistive behaviour characterized by very stable electrical response to applied stretching up to 50% deformation, high sensitivity especially at low deformations with gauge factor values up to 11.7 and fast response time down to 500 ms when stretched at 100 mm/min rate at 2.5% strain. Overall, the results demonstrate that rGO/PU coated fabrics are very promising wash-durable electrically conductive e-textiles with improved comfort, enhanced thermal conductivity for possible thermal therapy applications, and piezoresistive properties for sensing applications as human motion monitoring.

Keywords Reduced graphene oxide · Coating · Piezoresistive sensor · Wash-durable · Cotton textile

Supplementary Information The online version contains supplementary material available at https://doi.org/10.1007/s10570-023-05042-w.

F. Olivieri · F. De Falco · R. Avolio · I. Bonadies · R. Castaldo (✉) · M. Cocca · M. E. Errico · G. Gentile
Institute of Polymers Composites and Biomaterials, National Research Council of Italy, Via Campi Flegrei, 34, 80078 Pozzuoli, NA, Italy
e-mail: rachele.castaldo@cnr.it

G. Rollo · M. Lavorgna
Institute of Polymers Composites and Biomaterials, National Research Council of Italy, Via Previati 1, 23900 Lecco, Italy

M. Lavorgna
Institute of Polymers Composites and Biomaterials, National Research Council of Italy, P. Le Enrico Fermi 1, 80055 Portici, NA, Italy

Introduction

Electrically conductive textiles have acquired significant interest for their applicability as wearable electronic devices such as strain/pressure sensors (Kim et al. 2018; Zhu et al. 2021), wearable heaters (Souri and Bhattacharyya 2018), temperature or humidity sensors (Zhou et al. 2017; Zheng et al. 2022). In particular, strain and pressure sensors can be employed

to monitor human motion to detect physical and physiological activities of humans, to provide real time monitoring for the diagnosis of stress, for ongoing health care or for correcting posture. These types of sensors require high sensitivity for small deformations, and it would be desirable that they have high stability over usury, humidity and washing cycles. At the same time, desirable features for wearable sensors are the breathability and the flexibility of the substrate. Natural materials such as cotton, hemp and wool offer several advantageous features such as natural abundance, environmental friendliness and cost effectiveness. In particular, cotton is made by cellulose, which is the most abundant organic compound on Earth, and is very favoured by its good air permeability, flexibility, softness and comfort, which make cotton fabric comfortable and breathable to wear when compared to synthetic fabrics (Ren et al. 2017; Chen et al. 2021). Also, cotton possesses numerous hydroxyl groups on the surface, which can help finishing treatment, promoting effective binding with active materials.

Indeed, electrically conductive fabrics are made by the combination of conductive materials with textiles and represent a widely exploited class of systems for application in several fields, such as sensing (Ko et al. 2018), energy storage (Bao and Li 2012), biomedicine (Eskandarian et al. 2020; Rollo et al. 2022) and e-textiles (Wang and Facchetti 2019). However, the traditional metal-inks widely used to realize conductive textiles can be toxic, expensive, non-environmentally sustainable and may require high temperature and processing costs, all these factors severely limiting their range of applications (Irimia-Vladu et al. 2012; Karim et al. 2019; Afroj et al. 2020). Alternative strategies to impart electrical functionality to textiles range from in-situ polymerization of conductive monomers (Oh et al. 1999; Dall'Acqua et al. 2006) to the application of conductive coatings onto the fabric (Shateri-Khalilabad and Yazdanshenas 2013; De Falco et al. 2019b). While the former usually requires complex processes, expensive materials and pre-functionalization of the fibers, the latter is considerably more versatile. Indeed, the application of functional layers, including nanocomposite or hybrid coatings, onto fabric substrates allows to significantly widening the range of functional properties that can be imparted to textile surfaces. Highly conductive heaters, made of natural fibre-based fabrics coated with a simple, environmentally friendly and scalable process based on stir coating and dip coating were realized using highly conductive ink based on graphene nanoplatelets and carbon black particles (Souri and Bhattacharyya 2022). Also, conductive textiles with ultrahigh resistance to rubbing and washing were realized with a single-walled carbon nanotubes/polyamide coating on cotton or PET fabrics (Zhu et al. 2021). Nevertheless, to obtain high electrical conductivity and durability, it was necessary to apply high amount of nanocomposite coating (up to 40 wt% in the last case), and these amounts significantly affect the hand of the textiles and their flexibility, limiting their possible use for wearable applications. On the contrary, thin functional coatings would preserve the typical characteristics of the fabrics, such as their wearability, high flexibility and lightness, as well as their breathability (Sahito et al. 2015; Yetisen et al. 2016; Shathi et al. 2020).

Reduction of graphene oxide (GO) is an easy way to obtain uniform and thin conductive coatings on a wide range of substrates, such as textiles (Ergoktas et al. 2020). GO can be applied by several techniques, including spray coating (Shi et al. 2015), solvent casting (Hwang et al. 2021) and dip coating (Yaghoubidoust and Salimi 2019). Then, reduced graphene oxide (rGO) can be obtained by thermal annealing (Castaldo et al. 2019) or chemical treatments with proper reducing agents such as ascorbic acid (AA) (Castaldo et al. 2021) or hydrazine (Park et al. 2011). Chemical treatments have the advantage of preserving the carbon plane structure more efficiently than the thermal annealing processes, which induce the desorption of oxygen-containing functional groups from the GO planes. In particular, a combination of the two treatments demonstrated to be highly efficient for electrical conductivity (Gao et al. 2009; Pei and Cheng 2012). Specifically, rGO coating are very appropriate for cotton textiles, since the residual oxygen-containing functional groups are able to interact via hydrogen bonding with the hydroxyl functional groups of cellulose, ensuring excellent adhesion to the fabric (Karim et al. 2017). Also, rGO based coating are properly suitable for piezoresistive applications, being sensitive to mechanical or electrical stresses (Jiang et al. 2019; Hong et al. 2021).

Nevertheless, the co-presence of the required mechanical and electrical properties for piezoresistive materials, combined to high resistance to washings,

keeping unaltered the breathability and the hand of wearable textiles, is a complex issue and still few papers are focused on the peculiar combination of all these aspects (De Falco et al. 2019a; Li et al. 2019). Recently, an approach based on the application of a rGO coating followed by the deposition of an external Ni or Cu layer by vacuum arc deposition has been proposed to realize cotton substrates suitable for pressure sensing (Chen et al. 2021). However, to obtain very low surface resistivity, the proposed method is based on the application of a thick rGO layer whose electrical conductivity is further improved by the continuous metal layer.

In this work, conductive coatings for cotton textiles were designed and realized through an easy and scalable process, based on GO deposition by dip-coating, followed by eco-friendly reduction induced by ascorbic acid coupled to thermal treatment. In addition, a thin polyurethane layer was applied, with the objective of improving the coating durability and promoting enhanced piezoresistive performances. The coatings structure, morphology and durability were evaluated. Then, the realized systems were characterized by evaluating their breathability and thermal conductivity to assess their comfort and thermal properties, and by electromechanical tests, to assess their functionality as piezoresistive sensing textiles.

Experimental section

Materials

Cotton fabric (cotton, plain wave, weight 230 g/m^2, thickness about 1 mm, thread density 730 yarns/m), purchased by a local distributor, was employed as substrate. Graphene oxide (GO) water dispersion (dry content 0.45 wt%) was obtained by Nanesa Srl (Arezzo, Italy). Polyurethane (PU) water dispersion (Idrocap 994) was purchased by Icap-Sira Srl (Parabiago, Milano, Italy). Ascorbic acid (AA) and all other chemicals were purchased by Merck Life Science Srl (Milano, Italy) and used without further purification.

Coating deposition

Before coating applications, cotton fabrics were cleaned by immersing them in diethyl ether anhydrous for 10 min. Then, cotton fabrics specimens (about 10×10 cm^2) were dip-coated with a GO/AA aqueous dispersion with a GO dry content of 0.45 wt% and a GO:AA weight ratio 1:10. The impregnation was considered completed once, after blotting on filter paper to remove the excess dispersion, the fabrics reached a constant weight gain. Then, the fabrics were dried at room temperature overnight. These samples were coded GO/AA_cotton. GO/AA_cotton fabrics were kept in oven at 150 °C for 2 h, in order to promote chemical and thermal GO reduction. After that, the obtained fabrics were washed with distilled water in order to remove AA and dried at room temperature overnight. The obtained fabrics were coded rGO_cotton.

A further cotton specimen was impregnated with a 0.45 wt% GO dispersion as previously described, but without using AA. This sample, coded GO_cotton, was not subjected to thermal reduction, and was used for comparison in Raman analysis to assess the reduction of GO to rGO.

The rGO_cotton fabrics were impregnated in three PU water dispersions previously diluted with distilled water at different dry contents, namely 0.5, 1.0 and 2.0 wt%. The impregnations were performed similarly to the GO/AA impregnations. The obtained samples were dried at room temperature overnight and coded rGO_PUx_cotton, where x indicates the corresponding PU dispersion dry content.

Characterization

Fourier transform infrared spectroscopy (FTIR) analysis was performed on cotton, rGO_cotton, rGO_PU0.5_cotton, rGO_PU1_cotton, rGO_PU2_cotton and, for comparison, on a PU film obtained by casting evaporation from the PU solution. Measurements were performed in attenuated total reflectance (ATR) with a PerkinElmer Spectrum One FTIR spectrometer, using a resolution of 4 cm^{-1} and 32 averaged scans.

Raman spectra were performed on cotton, rGO_cotton, rGO_PU0.5_cotton, rGO_PU1_cotton, rGO_PU2_cotton. Measurements were performed with a Horiba-Jobin Yvon Aramis Raman spectrometer operating with a diode laser excitation source limiting at 532 nm and a grating with 1200 grooves mm^{-1}. The 180° back-scattered radiation was collected by an Olympus metallurgical objective (MPlan 50X, numerical aperture = 0.50) and with confocal and

slit apertures both set to 400 mm. The radiation was focused onto a Peltier-cooled charged-coupled device detector (Synapse Mod. 354,308) in the Raman-shift range 3500–800 cm^{-1}. Spectral deconvolution of unresolved peaks was performed using the software Grams/8.0AI, using a Lorentzian function. By a curve fitting of the data, height, area, and position of the individual components were evaluated.

Washing tests were performed on rGO_cotton, rGO_PU0.5_cotton, rGO_PU1_cotton and rGO_PU2_cotton at lab scale using a Gyrowash equipment (James H. Heal & Co). The fabric samples were placed in the steel containers of the Gyrowash, along with 10 steel balls. The liquor was distilled water. The liquor ratio (liquor:specimen) was 150:1 vol/wt, corresponding to 150 mL of liquor per gram of fabric (De Falco et al. 2018). A total of 10 subsequent washing cycles, each lasting 45 min, were performed on the fabric samples. The first 5 cycles were performed at 20 °C ("cold" cycles), and the following 5 cycles were performed at 40 °C ("hot" cycles). Between consecutive washings, fabric samples were dried at room temperature.

Morphological analysis of cotton, rGO_cotton and rGO_PU2_cotton samples before and after the 10 washing cycles was performed by scanning electron microscopy (SEM) using a FEI Quanta 200 FEG SEM in high vacuum mode. Before SEM observations, samples were mounted onto SEM stubs by means of carbon adhesive disks and sputter coated with a 5–10 nm thick Au–Pd layer. All the samples were observed at 10 kV acceleration voltage using a secondary electron detector. The rGO/PU coating structure on the rGO_PU2_cotton sample was also investigated by transmission electron microscopy (TEM). A small rGO_PU2_cotton specimen was embedded with an epoxy resin (Epoxy-Embedding kit 45,359, Sigma-Aldrich). Ultrathin sections of the embedded sample was obtained through a Leica UC7 ultramicrotome (nominal thickness = 130 nm) and collected on TEM copper grids. TEM observations were performed in bright-field mode with a FEI Tecnai G12 Spirit Twin microscope (LaB6 source) equipped with a FEI Eagle 4 k CCD camera, using an acceleration voltage of 120 kV.

Surface resistivity (ρ_S) measurements were performed on cotton, GO/AA_cotton, rGO_cotton and rGO_PUx_cotton samples using a Keithley Electrometer/High resistance meter, Model 6517A, with a two-point probe in alternated current, applying 100 V voltage. Tests were registered in triplicate; average results are reported. Before testing, the fabric samples were conditioned at 25 °C and 50% RH.

Breathability tests were performed on cotton, rGO_cotton and rGO_PU2_cotton through the upright ASTM E96 cup standard at 25 °C and 50% RH, in triplicate.

Thermal conductivity (λ) of cotton, rGO_cotton and rGO_PU2_cotton was measured at 25 °C by using the multipurpose apparatus ISOMET Applied Precision. For each sample, λ values were measured on overlapped fabrics (80 mm × 80 mm lateral size) to reach an overall thickness of 1.5 cm, in triplicate.

Then, the heating behaviour of cotton, rGO_cotton and rGO_PU2_cotton was qualitatively evaluated placing the samples in contact with a localized heating source and analysing the sample temperature by an infrared thermal camera. In detail, the central parts of fabric samples (50 mm × 50 mm in size) were positioned on the square base (10 mm × 10 mm in size) of an aluminium parallelepiped whose opposite square base was heated at 50 °C with a heating plate. The fabrics temperature was monitored with an infrared thermal camera (FLIR Systems, Thermo Vision A40M) until a plateau temperature was reached (about 300 s). Analysis of the collected images allowed to evaluate the heating rate of cotton, rGO_cotton and rGO_PU2_cotton in correspondence of the heating source (considering a circular area of 4 mm diameter) and on areas of the fabric located at 20 mm from the center of the heating source.

Piezoresistive properties of rGO_cotton and rGO_PU2_cotton fabrics were evaluated by combined tensile tests, performed through an Instron 5564 dynamometer, and current measurements, performed by a Keythley 2450 multimeter. In details, a 15 yarns-wide fabric sample with a gauge length of 2 cm was mounted between two non-conductive clamps of the dynamometer and conductive copper tape was used to connect the sample extremities to the multimeter. Therefore, cyclic tensile tests were conducted at 10 mm/min deformation rate, with 10 cycles at each deformation step. For all samples, an initial preload corresponding to 1 mm of deformation was imposed. Incremental deformation steps ranging from 2.5 to 50% were imposed in this way: in the range 2.5—20%, deformation was increased with a 2.5% step; in the range 20—30%, deformation was increased

with a 5% step; in the range 30%—50%, deformation was increased with a 10% step. After each step ranging from 5 to 40%, a 2.5% deformation step was repeated before passing to the next deformation step. Contemporarily to the tensile tests, a 3 V voltage was applied at the extremities of the sample and a current measurement test was set in the two-electrode configuration. To further evaluate the piezoresistive performances of rGO_PU2_cotton, a similar test was performed on this sample with 100 and 50 consecutive cycles at 15% and 20% deformation respectively. Then, the effect of the strain rate on the response and recovery time of rGO_PU2_cotton at variable deformation was assessed repeating the 2.5% and 15% stretching/release cycles also at 100 mm/min; the response and recovery time of rGO_PU2_cotton were evaluated for these deformations both at 10 mm/min and at 100 mm/min. A durability test was performed by subjecting the rGO_PU2_cotton sample to 1000 consecutive stretching/release cycles at 100 mm/min. The hysteresis in relative current change in response to deformation was evaluated for the 10th, 100th and 1000th deformation cycles. These tests were performed at 25 °C and 50% RH.

The effect of humidity on the piezoresistive response of the rGO_PU2_cotton sample was investigated by performing electromechanical tests on rGO_PU2_cotton at variable water content. First, the rGO_PU2_cotton sample was subjected to 10 stretching cycles at 15% strain and 10 mm/min strain rate at room humidity (50% RH, *dry* cycles); then, the sample was impregnated with distilled water and the test was prolonged for further 10 *wet* cycles.

Finally, the applicability of the rGO_PU2_cotton system as a wearable sensor for human motion monitoring was qualitatively evaluated. A rGO_PU2_cotton fabric (approximate size 15×10 cm^2) was applied onto a high stretchable cotton sport shirt, in the position corresponding to the right elbow. After the shirt was worn, the rGO_PU2_cotton was connected to the Keythley 2450 multimeter and, applying a 3 V voltage, the current was measured at different arm bending angles.

Results and discussion

Reduced graphene oxide thin coatings were obtained on cotton fabrics through a simple dip coating process followed by a combined chemical-thermal reduction procedure. As shown in Fig. 1, cotton fabric was treated with a GO/AA dispersion by dip-coating. The

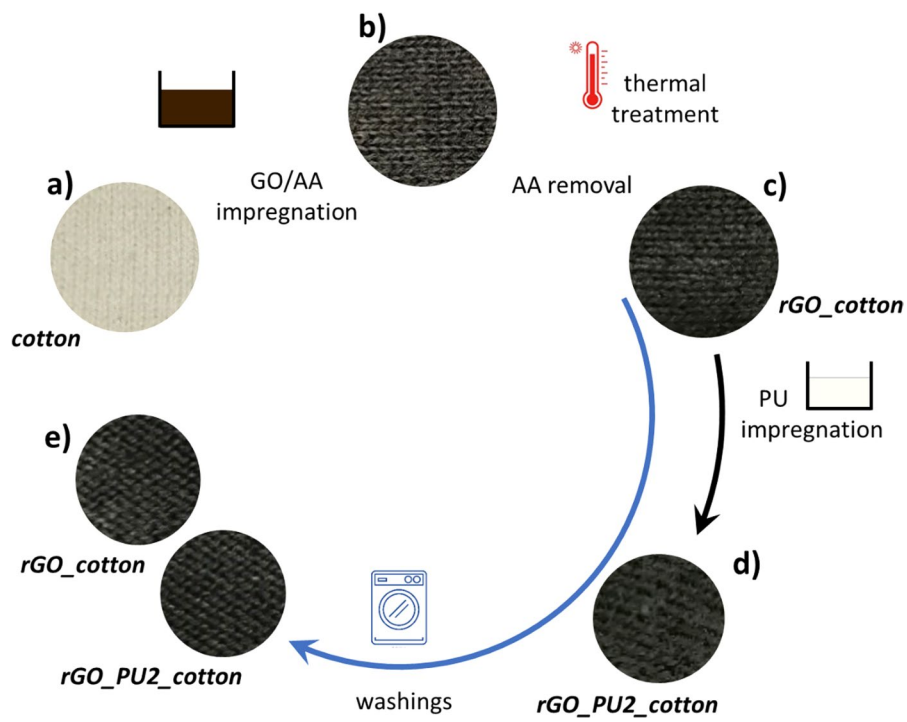

Fig. 1 Overall scheme of the work, showing the images of cotton fabric (**a**), cotton fabric after GO/AA impregnation (**b**), rGO_cotton (**c**) and rGO_PU2_cotton before (**d**) and after 10 washing cycles (**e**)

dipping treatment was prolonged for about 1 min until, after blotting on filter paper, the fabric weight gain was constant, and the specimens gained about 200% of their original weight. Then, after drying, the GO/AA-treated cotton substrates were subjected to a thermal treatment in order to obtain a combined chemical/thermal reduction of the graphene coating, and washed with distilled water to remove unreacted AA and AA by-products. By considering the GO content of the absorbed water dispersion, the applied rGO phase resulted 9.0 mg/g of cotton, or, expressed in weight per fabric surface, 2.07 g/m^2.

With the objective of improving the coating durability and the piezoresistive performances of the fabrics, an external polyurethane layer was applied through a second dip-coating treatment in PU water dispersions at varying PU dry contents. In this case, the rGO-coated fabrics gained about 100% of their original weight. Therefore, considering the PU dry content of the impregnation baths, rGO_PU0.5_cotton, rGO_PU1_cotton and rGO_PU2_cotton were coated with nominal amounts of 1.15, 2.30 and 4.60 g of PU per square meter of fabric, respectively. All the fabric samples, including that with the maximum amount of applied PU, rGO_PU2_cotton, did not show a significant change of the hand of the fabric, neither of its morphology, as shown in Fig. 1d for the sample with the highest amount of PU, rGO_PU2_cotton. On the contrary, further increasing the dry content of the PU water dispersion used for the dip coating process led to significant modification of the hand of the textile with respect to pristine cotton, with a pronounced tactile feeling of stiffness and heaviness of the fabric.

The morphology of the coated cotton substrate at different stages of the process is illustrated in Fig. 2. The differences between untreated cotton and cotton after GO/AA impregnation are evident. Large amounts of GO/AA film, pointed with yellow arrows in Fig. 2c, d, are deposited on the surface of cotton fabric, fully covering the cotton fibers. The GO/AA phase forms a continuous film embedding adjacent fibers and masking the surface of the fibers. This morphology is indistinguishable from that shown by GO/AA treated cotton after the thermal reduction treatment. To be noticed is that at this stage, the textile hand is highly affected by the significant amount of applied AA, that, being ten-fold the amount of GO, corresponds to about 21 g of AA per square meter of cotton fabric. After AA removal by washing with distilled water, the rGO coated fabric (rGO_cotton) shows a different morphology (Fig. 2e,f). The fibers are much more clean due to removal of the AA phase, and a very thin and homogenous rGO layer covers the cotton fibers, as evidenced by protruding platelets (pointed by orange arrow in Fig. 2f), not affecting significantly the morphology of the fibers. Upon application of the PU coating, the morphology of the fibers shows further peculiar features. Thin PU films bridging adjacent fibers can be observed (evidenced by green arrows in Fig. 2g,h), without masking, however, the presence of rGO platelets, evidenced with orange arrows, and imparting a smoother morphology to the fibers. The uniformity of rGO and rGO/PU coatings on a large scale is revealed by low magnification images shown in Figure S1.

TEM analysis was used to better investigate the applied rGO/PU coating. Bright field TEM images of rGO_PU2_cotton are reported in Fig. 2i-k. The TEM micrograph at lower magnification clearly shows the cross-section of a cotton fiber fully coated with a dense external layer attributed to a composite rGO/PU coating. Indeed, progressively increasing the magnification, a compact PU layer is observed, whose overall thickness, evidenced by the green arrow in Fig. 2k, is in the range 40–65 nm, embedding high contrast platelets attributed to stacked rGO sheets.

ATR-FTIR spectra of pristine cotton and cotton fabrics coated with rGO and PU are shown in Fig. 3a. Cotton shows the typical cellulose absorption signals: O–H stretching in the 3650–3000 cm^{-1} range, O–H in-plane bending at 1335 and 1203 cm^{-1}, C-H stretching in the 2980–2800 cm^{-1} range, C-H wagging at 1427 and 1314 cm^{-1}, C-H bending at 1730 and 1360 cm^{-1}, C-H deformation stretch at 1280 cm^{-1}, C-O stretch in the range 920–1060 cm^{-1}, C–O–C asymmetric stretching at 1104 and 1160 cm^{-1}, and a broad peak at 1640 cm^{-1} due to adsorbed water molecules (Roeges 1994; Chung et al. 2004). In the rGO_cotton spectrum all the cotton signals are still evident, due to the very thin nature of the rGO coating. Nevertheless, the presence of the rGO layer is not clearly detected, as rGO mainly induces a lowering of the baseline, more significant at lower wavenumbers. On the contrary, ATR-FTIR analysis was useful to confirm the homogeneity of the applied external PU layer. The spectra of the rGO_PU coated fabrics show

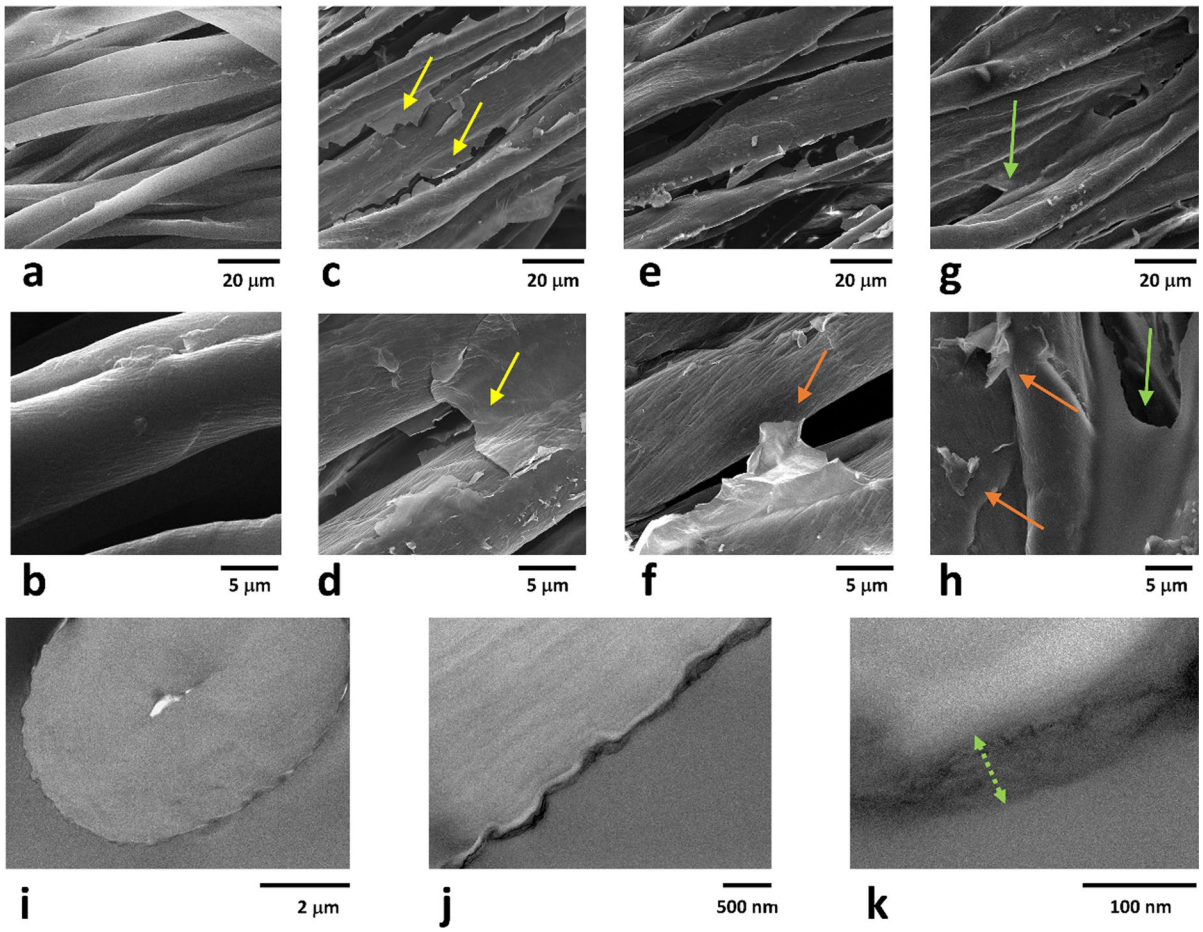

Fig. 2 SEM images of cotton (**a**, **b**), cotton impregnated with GO/AA (**c**, **d**), rGO_cotton (**e**, **f**) and rGO_PU2_cotton (**g**, **h**) fabrics; Bright field TEM images of rGO_PU2_cotton (**i**, **j**, **k**)

absorption bands typical of the polyurethane phase, such as the C = O stretching signal at 1740 cm^{-1}, the aromatic C–C stretching at 1530 cm^{-1}, the C–O–C stretching signal at 1243 cm^{-1} and the C-H bending at 790 cm^{-1} (Trovati et al. 2010). For each sample, the analysis of different areas of the sample does not show significant change of the ratio between the peak centred at 1243 cm^{-1}, attributed to PU, and the peak centred at 1020 cm^{-1}, attributed to cotton cellulose, indicating the homogenous distribution of the external PU coating on the rGO_cotton surface. Moreover, the intensities of the PU absorption bands progressively increase along the series rGO_PU0.5_cotton—rGO_PU1_cotton—rGO_PU2_cotton, confirming that the increase of the dry content of the PU water dispersion induces an increase of the amount of applied PU on the fabric.

Raman spectra of GO and rGO coated fabrics allowed to reveal the presence of GO and its reduction after the combined chemical/thermal treatment. Raman spectra of cotton, GO_cotton, rGO_cotton and rGO_PU2_cotton fabrics are shown in Fig. 3b. The typical GO bands D (centred at 1350 cm^{-1}) and G (centred at 1590 cm^{-1}) are well evident in the fabric coated with GO. The spectrum of the rGO_cotton sample shows an increase of the I_D/I_G ratio from 0.85 (GO_cotton) to 0.99 (rGO_cotton), this phenomenon being often associated to GO reduction, ascribed to an increased degree of disorder due to the new defects and vacancies generated during the reduction process (Tuinstra and Koenig 2003). Also, the G band of rGO_cotton shifts to lower wavenumbers in comparison to GO_cotton, and the D' band (centred at 1612 cm^{-1}), associated to

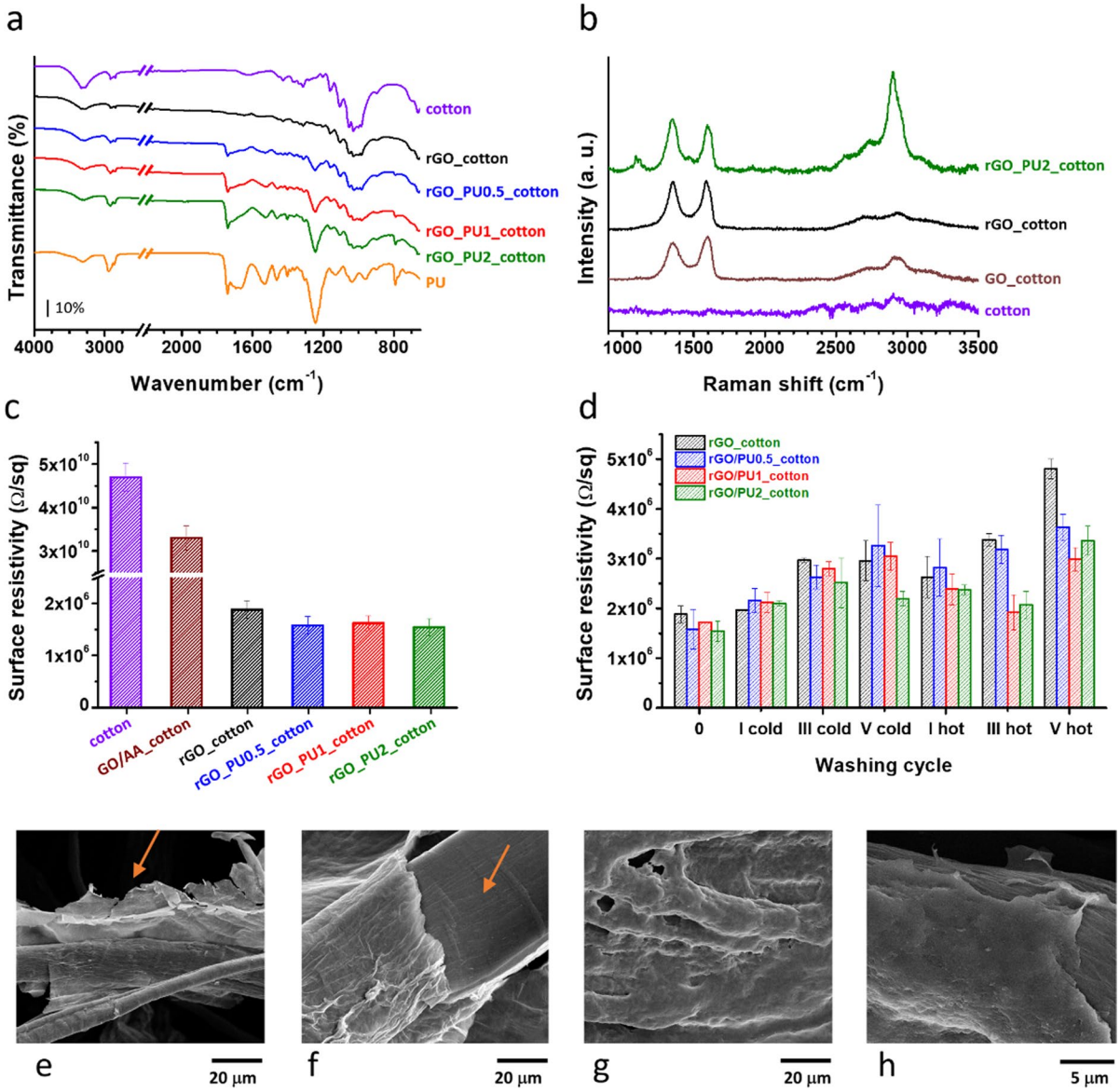

Fig. 3 FTIR spectra of cotton, rGO and rGO_PU coated cotton fabrics and PU film (**a**), Raman spectra of cotton, GO, rGO and rGO_PU2 coated cotton fabrics (**b**), surface resistivity of cotton and coated fabrics (**c**) and surface resistivity of coated fabrics depending on washing cycles (**d**); SEM images of rGO_cotton (**e**, **f**) and rGO_PU2_cotton (**g**, **h**) after the 5th hot washing cycle

disordered carbon, appears as a shoulder on G band (Castaldo et al. 2021). At higher wavenumbers, the overtone 2D band (2700 cm^{-1}) and the D + G band (2900 cm^{-1}) are partially superposed to the cotton absorption signals at 2750 cm^{-1} and 2900 cm^{-1}. After the deposition of the PU layer on the rGO_cotton fabric, the presence of rGO is still detectable in the Raman spectrum of rGO_PU2_cotton, where the typical rGO signals are partially overlapped with the PU absorption bands in the 1000–1800 cm^{-1} region, where the bands associated to the C–N stretch (at about 1530 cm^{-1}) and to the ester C = O (at about 1730 cm^{-1}) are centred (Parnell et al. 2003), and in 2500–3200 cm^{-1}region, where the C-H stretching band of poly(ether urethanes) are located (Roohpour et al. 2009).

The effect of the reduction process on the surface electrical resistivity of the fabric samples is shown in Fig. 3c. Upon GO/AA impregnation, the cotton surface resistivity, ρ_S, passes from 4.7 $\cdot 10^{10}$ to 3.3 $\cdot 10^{10}$ Ω/sq. Then, after the thermal treatment of the fabrics and AA removal, ρ_S decreases of four orders of magnitude, down to about 1.9 $\cdot 10^{6}$ Ω/sq. Interestingly, although pristine PU has a very high surface resistivity (1.6 $\cdot 10^{16}$ Ω/sq), its application on the surface of rGO_cotton does not significantly affect the electrical conductivity of the fabrics, irrespectively of the PU amount. This phenomenon can be explained considering that, once the external PU layer is applied onto the rGO_cotton sample, the absorption of the PU water dispersion by the cotton substrate induces the formation of a nanocomposite PU/rGO coating (see also Fig. 2i-k) that, containing stacked rGO platelets that well percolate the coating structure, keeps the electrical conductivity of the fabric comparable to that shown by the fabric coated with only rGO (De Falco et al. 2019b).

The washing cycles on rGO_cotton and rGO_PU coated fabrics did not have significant effect on the visual appearance of the samples, as shown in Fig. 1e for rGO_cotton and the sample containing the highest amount of PU, rGO_PU2_cotton. The effect of the washing cycles on the electrical properties of the samples was evaluated by measuring the electrical resistivity of the coated fabrics after 1, 3 and 5 subsequent washings at 20 °C ("cold" cycles) and then after 1, 3 and 5 subsequent washings at 40 °C ("hot" cycles). As shown in Fig. 3d, the surface resistivity of the coated samples slightly increases during the washings, although remaining in the same order of magnitude. Nevertheless, it is interesting to note that, on average, the samples coated with higher amount of PU (rGO_PU1_cotton and rGO_PU2_cotton) show the lowest surface resistivity values (up to 3 $\cdot 10^{6}$ Ω/sq), while rGO_cotton and rGO_PU0.5_cotton show the highest surface resistivity values, with rGO_cotton reaching the maximum value of 4.8 $\cdot 10^{6}$ Ω/sq at the 10th washing cycle. Hence, resistivity measurements performed after multiple washings of the fabrics demonstrate that the external PU coating plays an important role in protecting the rGO percolating network during washings, also in comparison to other protective coatings developed for conductive cotton-based textiles (Table 1). This protective effect of the external PU coating was confirmed by evaluating SEM micrographs of rGO_cotton and rGO_PU coated fabrics after the washing cycles. Indeed, after the 5th hot washing cycle, the rGO_cotton sample showed detachment phenomena of rGO sheets and areas of cotton fibres that resulted uncoated (evidenced with orange arrows in Fig. 3e,f whereas an almost undamaged PU layer was found on rGO_PU2_cotton (Fig. 3g,h).

Breathability of rGO_cotton and rGO_PU2_cotton was evaluated to assess the comfort properties of the treated textiles. As already evidenced by SEM analysis, the rGO and rGO_PU coatings do not clog the woven structure of the pristine fabric. This phenomenon was quantitatively confirmed as breathability values resulted very close for all samples, from 0.95 ± 0.05 kg/m^2 d for the pristine cotton fabric, to 1.08 ± 0.06 kg/m^2 d and 1.11 ± 0.07 kg/m^2 d for rGO_cotton and rGO_PU2_cotton, respectively. Although not being very sizable, the slight increase of breathability registered upon coating with rGO and PU may be ascribed to a binding-like effect of the rGO and rGO/PU coatings on the cellulosic fabrics, which could compact the yarns constituting the woven structure, allowing a faster vapor flow.

The response to thermal solicitations of the coated fabrics was evaluated through thermal conductivity measurements combined with an infrared thermal camera analysis. Thermal conductivity measurements show higher thermal conductivity for rGO_cotton and rGO_PU2_cotton with respect to cotton, due to the presence of the rGO phase, with λ slightly increasing from 0.0918 ± 0.0014 Wm^{-1} K^{-1} for cotton to 0.0982 ± 0.0013 Wm^{-1} K^{-1} and 0.0947 ± 0.0020 Wm^{-1} K^{-1} for rGO_cotton and rGO_PU2_cotton, respectively. To be noticed is that these results are a measurement of the thermal conductivity of the sample either along the fabric surface, either across overlapped fabrics, as the analytical technique used for the measurement required the overlapping of several fabrics to reach the minimum thickness needed to obtain affordable measurements. This is also the reason of the slightly higher λ values obtained on our samples in comparison to data reported in literature for the surface thermal conductivity of cellulose fabrics, whose value depend on the grammage of the fabric and that range from about 0.030 to 0.088 Wm^{-1} K^{-1} (Stanković et al. 2008; Yu et al. 2019). In our system, the slight decrease of λ registered for rGO_PU2_cotton with respect to rGO_cotton is to be ascribed to

Table 1 Comparison of main features of cotton-based piezoresistive textiles

Substrate	Coating materials	Amount of conductive filler	Process	Electrical conductivity (S/m) or surface resistivity (Ω/sq)	Functional property	Stability after washing	Gauge factor	Response/recovery time	Reference
cotton	rGO/PU	0.9 wt% with respect to the coated substrate (grammage 2.07 g/m^2)	Dip coating, GO reduction by ascorbic acid, thermal treatment at 150 °C	~ 1.6 × 10^6 Ω/sq	Piezoresistivity (strain sensor); Localized heat conduction (thermal management)	Stable electrical response (1.6–3 × 10^6 Ω/sq) after 5 cold (20° C) and 5 hot (40 °C) washings	From 11.7 at 2.5% strain to 1.74 at 50% strain (tensile mode)	Strain rate 100 mm/min, 2.5% deformation: response 500 ms, recovery 330 ms	This work
Polyester/cotton fabric	rGO/phosphate flame retardant, adhesive finishing treatment	N. a	Dip coating, thermal treatment at 150 °C	~ 0.5 × 10^3 Ω/sq	Conductivity; flame retardancy	24 times increased electrical resistivity after 20 washing cycles	N. a	N. a	Zhao et al. (2020)
cotton or PET fabric	Single walled carbon nanotubes (SWNTs)/glucaric acid/chitosan	7.2 wt% with respect to the coated substrate (40 wt% of SWCNTs in the coating, which is 18 wt% of the coated textile)	Dip-coating, thermal treatment 180 °C	8.7–57 S/m	Piezoresistivity; Joule heating; EMI shielding	Electrical conductivity decreased by < 17% after 20 washing cycles	N. a	N. a	Zhu et al. (2021)
cotton	Thiol-modified rGO/PU	2 wt % rGO in 1 mm thick rGO/PU coating	Dip coating, thermal treatment at 110 °C	> 3 × 10^3 Ω/sq	EMI shielding	EMI shielding decreased by ~ 10% after 10 washings with detergent	N. a	N. a	Wang et al. (2019)
cotton	rGO	N. a	Coating by vacuum filtration, hot pressing at 180 °C	0.9 × 10^3 Ω/sq	Bending and compression strain sensing	0.9 × 10^3 Ω/sq to ~ 1.2 × 10^3 Ω/sq after 10 washings with detergent at 60 °C	N. a	N. a	Ren et al. (2017)

Table 1 (continued)

Substrate	Coating materials	Amount of conductive filler	Process	Electrical conductivity (S/m) or surface resistivity (Ω/sq)	Functional property	Stability after washing	Gauge factor	Response/recovery time	Reference
cotton	rGO/SWCNTs	N. a	Dip coating, GO reduction by hydrazine, thermal treatment at 80 °C	N. a	Bending strain and pressure sensing	Stable response after 10 washings	From 6.1 for strain range 3.3–5.5% to 1 for strain range 9.3–11.6% (bending mode)	N. a	Kim et al. (2018)
Cotton / wool combined with silicon eslastomer (Ecoflex) in a sandwich structure	Graphene nanoplatelets (GNP), Carbon black (CB)	N. a	Dip coating assisted by ultrasonication	N. a. (286.54 Ω and 232.15 Ω for coated cotton and wool)	Piezoresistivity; Joule heating	N. a	Up to 20.4 for strain 120–150%; 1.67 for strain 0–120%	N. a	Souri and Bhattacharyya (2018)
cotton	rGO/Cu; rGO/Ni	N. a	rGO deposited by vacuum filtration, Cu/Ni films coated by magnetic filtered cathodic vacuum arc deposition	2 Ω/sq; 7 Ω/sq	Piezoresistivity	Cu and Ni content decreased by 10% after 10 washings with detergent at 49 °C, resistivity increased from 2 to 4 Ω/sq and 7 to 9 Ω/sq	N. a	Under the pressure of 0.1 MPa: response 700 ms, recovery 1200 ms	Chen et al. (2021)

the presence of the PU phase, which partially shields rGO thermal conductivity. Nevertheless, rGO_PU2_cotton still shows thermal conductivity higher than pristine cotton.

To better elucidate the thermal behaviour of the samples in the directions perpendicular and parallel to the fabric surface, the heating behaviour of the fabrics was evaluated by an experimental setup based on an infrared thermal camera. IR images of samples put in direct contact with an underlying heated metal element (Fig. 4a) show that the pristine cotton fabric and the fabrics coated with rGO and with rGO/PU present different heating behaviours. In particular, the temperature profiles collected in the central fabric areas (Fig. 4c), i.e. those areas in correspondence of the underlying heating source, indicated by the blue circle in Fig. 4b, are significantly different for the three samples. While the recorded temperature of pristine cotton progressively increases from about 16.5 °C to 27.5 °C during the test, significantly higher temperature values are observed for rGO_cotton (final temperature at 300 s = 34.8 °C). Instead,

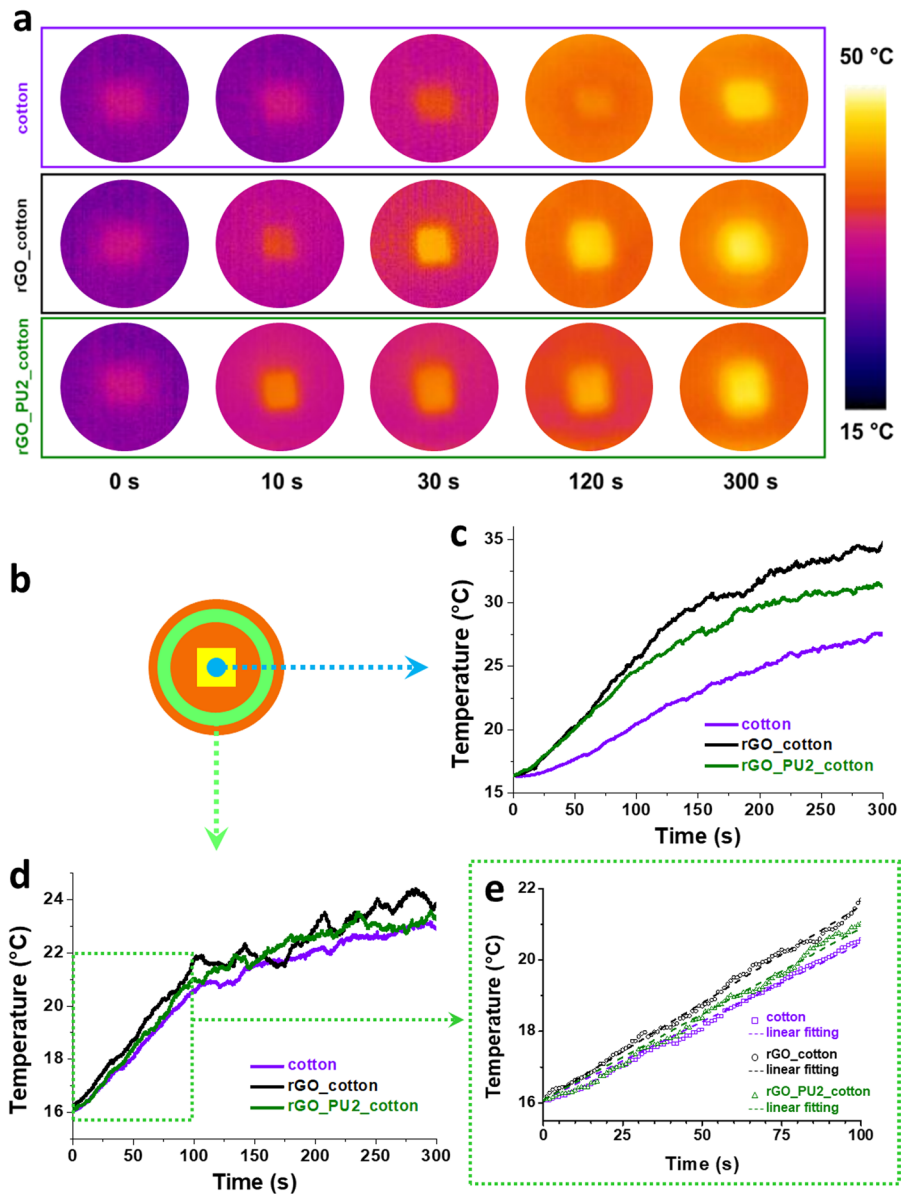

Fig. 4 Infrared thermal camera images of cotton, rGO_cotton and rGO_PU2_cotton subjected to localized heating (**a**); schematic representation of the analysed areas of the samples (**b**); temperature profiles of the samples in correspondence of the heating source, as indicated by the blue area in the scheme b (**c**) and on the peripheral region of the samples, as defined by the green ring in the scheme b (**d**, **e**)

rGO_PU2_cotton shows an intermediate final temperature, namely 31.3 °C. These results are in agreement with those obtained by the above discussed thermal conductivity measurements, confirming that the rGO coating effectively enhances the thermal conductivity of cotton and the presence of the additional protective PU phase only reduces the thermal conductivity of the rGO/PU coating. A significantly different behaviour can be observed for the three samples by evaluating the temperature profiles measured on the fabric surface areas at a fixed distance (20 mm) from the center of the heating source (see green circumference in Fig. 4b, d). In the analysed region, all samples show a comparable final temperature (about 23.8 °C) indicating that thermal dissipation phenomena due to heat exchange between the fabric and the environment start to prevail soon as one moves from the heating source. In those areas, the different thermal behaviour of the fabrics can be only appreciated by comparing the different slopes of the temperature profiles in the first part of the experiment (Fig. 4e), showing that rGO_cotton and rGO_PU2_cotton have a slightly higher heating rate up to about 100 s, while cotton shows the lowest heating rate. Overall, results show that rGO-coated cotton fabrics show interesting properties in terms of enhanced thermal conduction and possibility of confining the heat conduction through the fabric in correspondence of localized heating sources, for personal thermal management and thermal therapy applications (Repon and Mikučionienė 2021; Zhang et al. 2021).

Finally, the piezoresistive behaviour of the rGO_cotton and rGO_PU2_cotton fabrics was evaluated by means of combined tensile tests and current measurements. As shown in Fig. 5, when a constant differential electrical potential is set on the extremities of the coated fabrics and, contemporarily, a tensile stress is applied to the fabric, an increase in the current intensity is registered for both samples. In the same configuration, upon release of the tensile stress, the current intensity decreases for both samples. This phenomenon is to be ascribed to the major proximity of rGO conductive domains achieved in the coated fabrics in consequence to the tensile stress. Due to the tensile solicitation, the fabric yarns orientated along the tensile direction get closer, coming in contact with each other in multiple points. In this process, the conductivity of the fabric increases, while it decreased in response to the release of the applied strain. In both samples, the measured currents, in response to deformations from 2.5% up to 50% applied at 10 mm/min, range from 1×10^{-6} A to 3×10^{-6} A, and the registered load reaches about 10 N.

While the mechanical behavior of the two samples is comparable, the electrical response is deeply influenced by the PU layer. In fact, the current registered at zero deformation (I_0) for rGO_cotton fabric progressively decreases with the number of deformation cycles and with the increasing of the applied deformation, decreasing from about 1.5 µA to 1.0 µA (Fig. 5a-b), while for rGO_PU2_cotton I_0 is substantially constant during the test, around the value of 0.5 µA (Fig. 5c-d). This effect is to be ascribed to the fact that, upon stretching, the rGO coating covering the rGO_cotton fibers progressively loses its continuity, therefore inducing a decrease of the whole sample conductivity. Instead, the rGO_PU2 coated sample does not show a significant decrease of I_0 since it is characterized by higher elasticity, due to the polyurethane phase which preserves the coating integrity.

For deformations up to about 20%, both samples show increasing values of maximum current intensity (I_{max}) at subsequent deformation cycles. This trend comes to a plateau by increasing the number of cyclic deformations. Indeed, the increasing I_{max} for a fixed deformation is ascribed to the major proximity of conductive rGO domains, which is induced by the repeated approaching of neighboring coated yarns during cyclic tensile solicitations. I_{max} reaches a plateau value after a certain number of deformation cycles. In particular, the higher the deformation applied, the lower the number of cycles needed to reach an equilibrium current value. For example, rGO_PU2_cotton, solicited for 100 cycles at 15% deformation, reaches its I_{max} plateau value at about the 80th cycle (Figure S2). The same sample, solicited at 20% deformation, for the firsts cycle of deformation shows a maximum current of about $1.2 \cdot 10^{-6}$ A, and reaches the I_{max} plateau value at about 40 cycles (Figure S2). Then, at 25% and 30% deformation, quite constant I_{max} values are registered with just 10 cycles of deformation for both rGO_cotton and rGO_PU2_cotton samples.

A different phenomenon is observed at higher deformations, namely 40% and 50%. In these cyclic solicitations, I_{max} registered for rGO_cotton at the first cycle is respectively 9% and 10% higher than the plateau values registered in the following

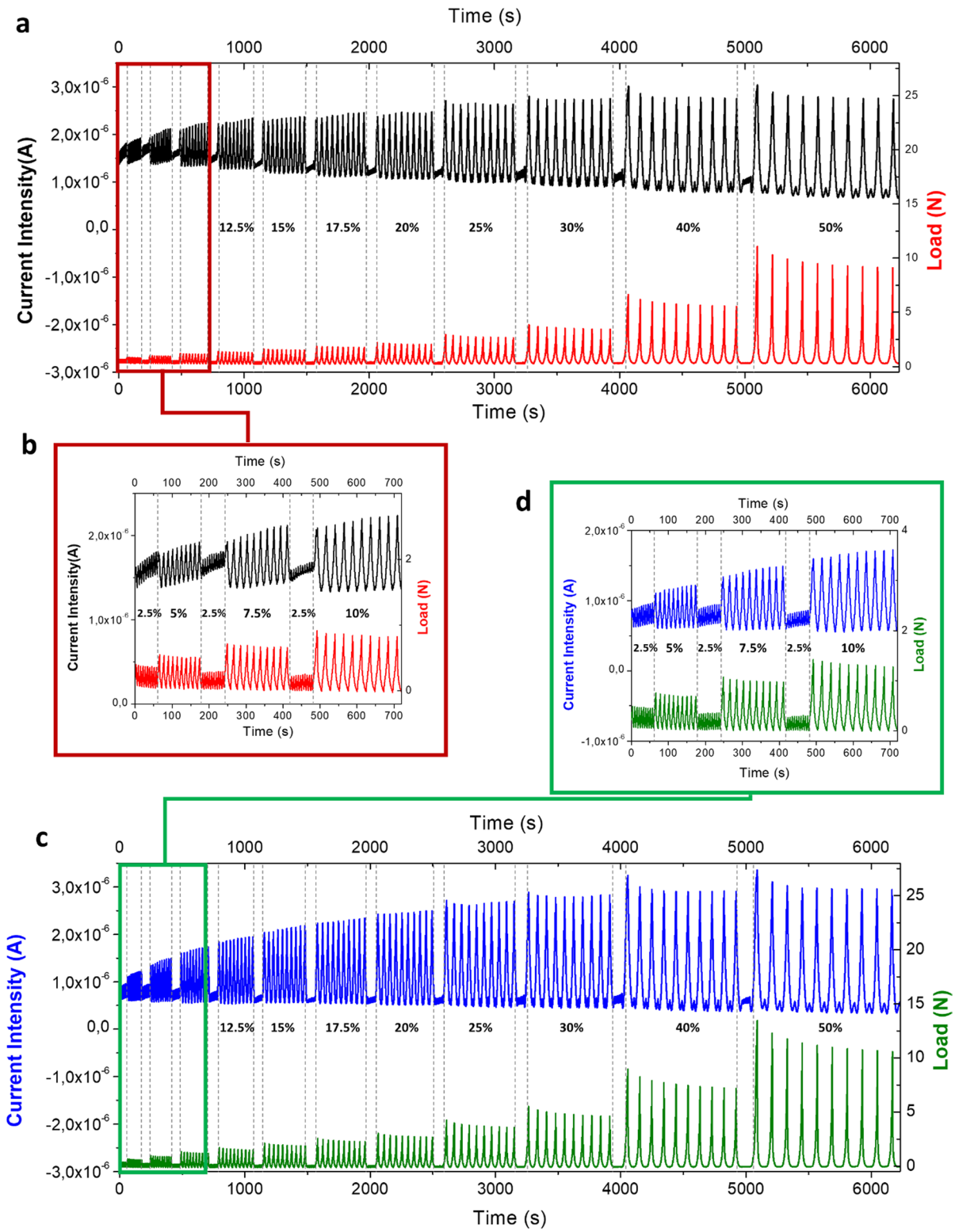

Fig. 5 Electromechanical cyclic tests of rGO_cotton (**a**, **b**) and rGO_PU2_cotton (**c**, **d**) at 10 mm/min

cycles, and for rGO_PU2_cotton it is about 10% and 14% higher than the corresponding plateau values. In this case, this behavior is to be ascribed to the irreversible stretching/damaging of the cotton fibers and therefore of the rGO coating covering the fibers. Subsequently to the first irreversible stretch, in the next deformation cycle the sample conductivity decreases to a lower value and, in the same way, the load registered for the sample decreases.

In general, for all ranges of deformation, a clear and noteworthy difference between rGO_cotton and rGO_PU2_cotton is represented by the extent of variation of between I_{max} and I_0, from here on denominated ΔI. At all deformations tested, rGO_PU2_cotton shows a significantly higher variation of ΔI with respect to rGO_cotton, demonstrating higher sensitivity in response to imposed deformations.

The samples electrical sensitivity to imposed deformations can be well displayed by the definition of the gauge factor (GF), which is an index of the piezoresistivity of a material and correlates the applied strain with the electrical resistance according to Eq. 1:

$$GF = \frac{\frac{\Delta R}{R_0}}{\frac{\Delta L}{L_0}} = \frac{\frac{\Delta R}{R_0}}{\varepsilon} \quad (1)$$

where ΔR (R_{max}—R_0) is the variation of electrical resistance due to deformation, R_{max} is the resistance of the sample at a fixed deformation, R_0 is the resistance exhibited by the material at zero deformation, and ε represents the strain.

Since the electric potential difference in the experiment is fixed, GF can be rewritten as:

$$GF = -\frac{\frac{\Delta I}{I_{max}}}{\varepsilon} \quad (2)$$

Usually, GF is a positive number, i.e. electrical resistance increases with applied strain increasing. However, for some materials, such as e-textiles, in which electrical resistance decreases with the alignment of conductive fibers toward the traction direction, GF is negative. Hence, in general, the piezoresistive sensitivity of the sample is directly correlated to the absolute value of the gauge factor (|GF|), being higher for higher |GF| values (Biccai et al. 2019).

|GF| values obtained from the electromechanical cyclic tests shown in Fig. 5 are higher for rGO_PU2_cotton than for rGO_cotton at all imposed deformation, revealing the generally higher sensitivity of rGO_PU2_cotton for piezoresistive sensing applications (see Fig. 6 and Table S1). For example, rGO_PU2_cotton and rGO_cotton show |GF| values of 11.7 ± 0.4 and 4.7 ± 0.4, respectively, at 2.5% deformation, and |GF| decreases exponentially with increasing the deformation extent for both samples, with an asymptotic trend reaching values of 1.74 ± 0.02 and 1.50 ± 0.01, respectively, at 50% deformation. In particular, rGO_PU2_cotton shows significantly higher sensitivity than rGO_cotton at lower deformations, as demonstrated by the higher slope of the |GF|(ε) curve of rGO_PU2_cotton and, also, rGO_PU2_cotton piezoresistive behaviour is characterized by higher accuracy (see R^2 in Fig. 6a), ensuring the strictly monotonic decrease of |GF| values with increasing the applied deformation. Therefore, the high |GF| values of rGO_PU2_cotton demonstrate high sensitivity for this sample as a strain sensor, also compared to literature cotton-based piezoresistive sensors which show much lower gauge factors in the same deformation range (Table 1).

Further characterization of the piezoresistive fabric rGO_PU2_cotton was aimed at evaluating the performances of the rGO_PU2_cotton as a strain sensor and its applicability as a wearable device.

The effect of water content on the piezoresistive properties of the coated fabric rGO_PU2_cotton was evaluated through combined tensile test and current measurements performed on the sample at 50% RH and after water uptake. A higher electrical response, from $5.3 \cdot 10^{-6}$ A in static condition (I_0) to $7.1 \cdot 10^{-6}$ A upon stretching (I_{max}), was promptly registered for the *wet* sample in comparison to the response registered in cycles at 50% RH. Indeed, it is reported that the conductivity of graphene-based materials increases due to the enhancement of ion conduction with increasing the ambient humidity (Yao et al. 2012). The barrier-free movement of water in graphene-based membranes has been demonstrated by Geim and collegues (Nair et al. 2012), showing that water molecules can readily intercalate the graphene structures. The effect of such intercalated water molecules is reflected on the proton conductivity of graphene oxide and reduced graphene oxide films (Ghosh et al. 2015). However, once subjected to the cyclic tensile

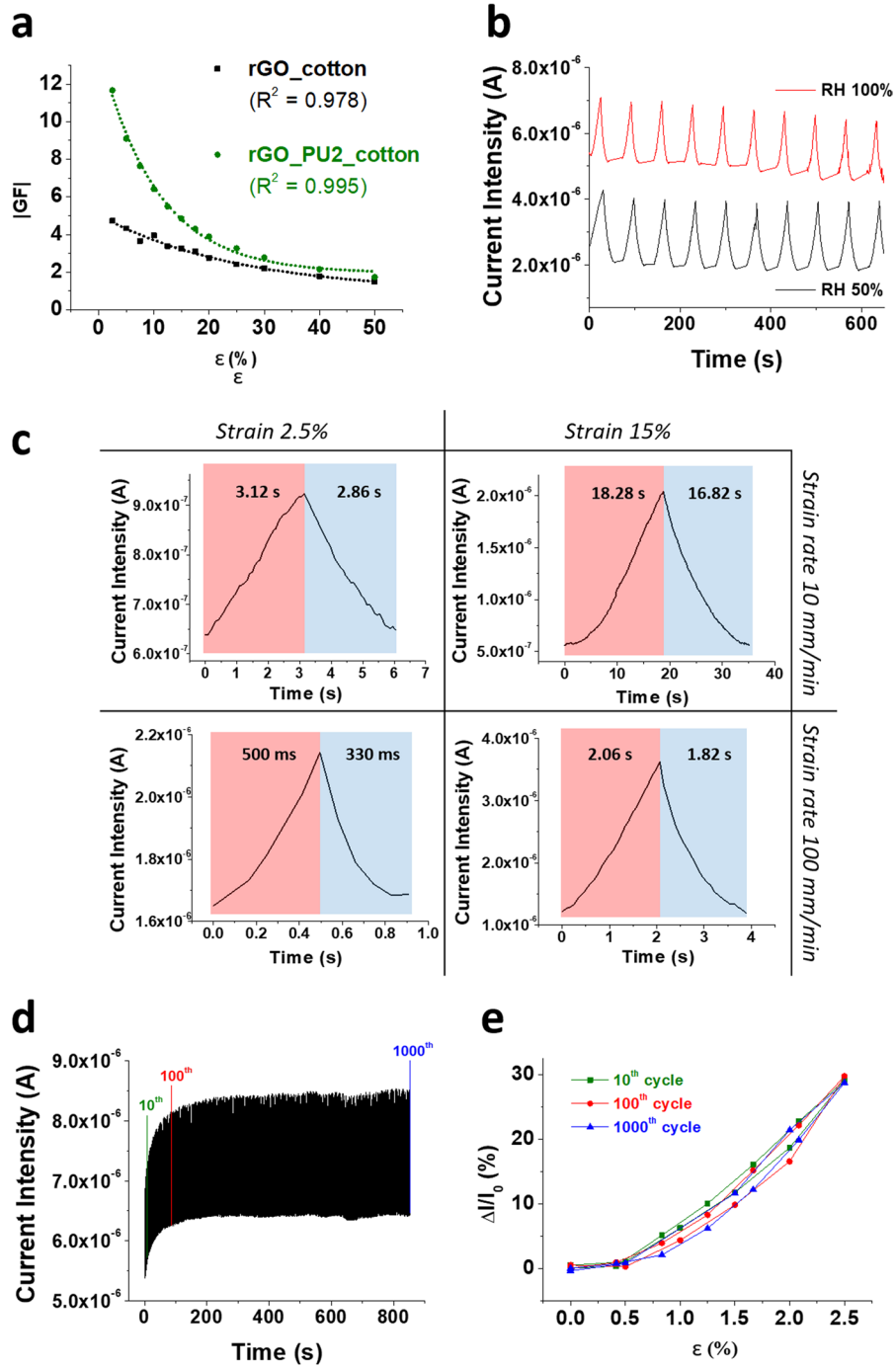

Fig. 6 Gauge factors values for rGO_cotton and rGO_PU2_cotton, with dotted fitting curves, related to electromechanical tests performed at 10 mm/min strain rate (**a**); electromechanical cyclic tests on rGO_PU2_cotton stretched at 15% strain and 10 mm/min strain rate, evaluated at 50% RH and 100% RH (**b**); response and recovery time of rGO_PU2_cotton stretched at 2.5% and 15% strain, 10 mm/min and 100 mm/min strain rate (**c**); rGO_PU2_cotton durability over 1000 stretch/release cycles at 2.5% strain and 100 mm/min strain rate (**d**); hysteresis curves of the 10th, 100th and 1000th stretch/release cycles corresponding to panel d (**e**)

test, the rGO_PU2_cotton sample showed a comparable cyclic response as the sample tested at 50% RH, with the conductivity of the fabric increasing in response to the applied strain and decreasing in response to the release of the applied strain, and with a comparable relative current change (Fig. 6b). A slight reduction of I_0 over the repeated cycles is ascribed to the progressive water evaporation from the fabric over time.

The response and recovery times of rGO_PU2_cotton to stretching and releasing were evaluated at different strains and at different deformation rates,

i.e. 2.5% and 15% strain, 10 mm/min and 100 mm/min strain rate. As expected, the response and recovery times are smaller when the fabric is stretched at higher strain rate. As shown in Fig. 6c, when the tensile deformations are applied at 10 mm/min, the response and release times of the sensor range from 2.86 to 18.28 s, while when the deformations are applied at higher rate, i.e. 100 mm/min, the response and release times significantly diminish, being in the range 330 ms–2.06 s. The fast response time of rGO_PU2_cotton at 100 mm/min strain rate is very relevant for applications of human body motion monitoring, and results to be in the range of rGO/metal ions coated cotton fabrics (Chen et al. 2021) (Table 1) and silver-coated nylon weft-knitted sensors (Li et al. 2021). Also, it is worth to notice that different strain rates have little effect on the relative electrical response of rGO_PU2_cotton, with I_{max}/I_0 decreasing of only 10% and 20% at 2.5% and 15% strain, respectively, with increasing the strain rate from 10 mm/min to 100 mm/min, which is appropriate to obtain a reliable response of the sensor.

The stability of rGO_PU2_cotton subjected to 1000 stretch-release cycles at 2.5% strain and 100 mm/min strain rate is shown in Fig. 6d. After a transient period in which the sensor reaches its plateau value, rGO_PU2_cotton reaches stable values of I_{max} and I_0, exhibiting high stability and low hysteresis (Fig. 6e). More importantly, the relative current ($\Delta I/I_0$) variation over the 1000 strain and release cycles is very low, as demonstrated by the similar trend of the 10th, 100th and 1000th hysteresis loops. Therefore, the multiple stretches do not destroy the functional coating developed in the rGO_PU2_cotton sensor and do not affect its repeatable response to stretching/releasing deformations.

The applicability of the rGO_PU2_cotton as a wearable sensor for human motion monitoring is shown in Fig. 7, where the coated fabric is shown applied to the motion of an arm. As the arm is straight and the sensor is at the release state, the current measured is around a value of 2.5 $\cdot 10^{-6}$ A (Fig. 7a); as the elbow is bent over so that the fabric is bent at 45°, 90° or 135° the current measured quickly rises to the higher values of 3.5 $\cdot 10^{-6}$ A, 6 $\cdot 10^{-6}$ A and 7.5 $\cdot 10^{-6}$ A, thus allowing to detect the movement entity, upon a proper calibration of the sensor.

Conclusions

In this work, reduced graphene oxide/polyurethane coatings were applied on cotton fabrics. Results show that all fabrics coated with very low amount of rGO and PU (2.07 g/m^2 and up to 4.60 g/m^2, respectively) are characterized by four orders of magnitude reduced surface resistivity with respect to the pristine cotton. All coated fabrics show limited changes of surface resistivity upon both cold and hot subsequent washings, and in particular, rGO_PU2_cotton is

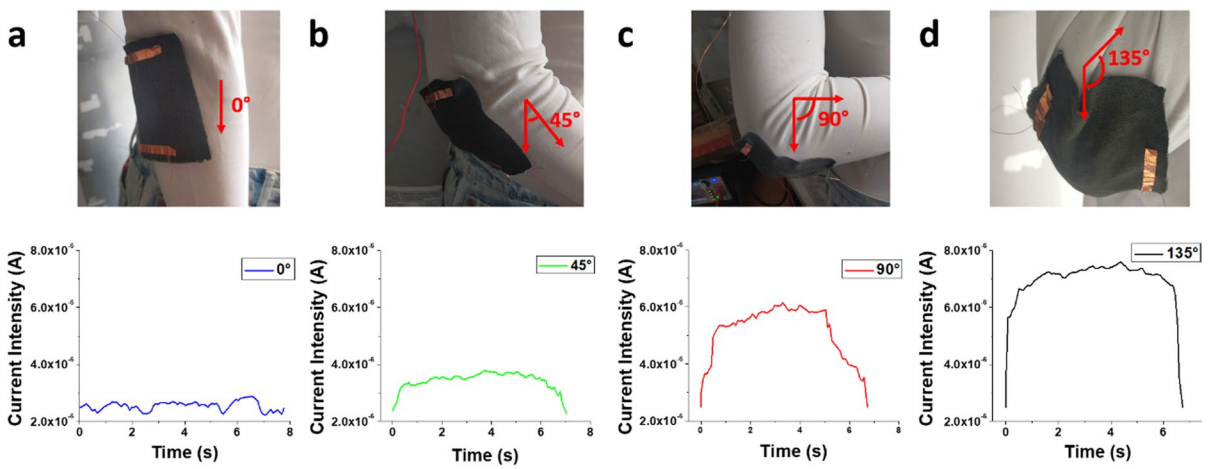

Fig. 7 Application of rGO_PU2_cotton as a wearable strain sensor, showing the electrical response of the sensor at release (**a**) and subjected to strain due to motion of an arm which induces the deformation of the piezoresistive fabric at 45° (**b**), 90° (**c**) and 135° (**d**)

characterized by the least variation of surface resistivity, demonstrating that the PU phase plays an important role in protecting the rGO coating during washing. Moreover, rGO_cotton and rGO_PU2_cotton show increased breathability and thermal conductivity with respect to cotton, demonstrating good comfort properties for wearable applications and good potentiality for personal thermal management. In particular, the evaluation of the thermal behaviour of the fabrics in the directions perpendicular and parallel to the fabric surface through infrared camera analysis indicated that the developed coatings are able to confine the heat conduction through the fabric in correspondence of localized heating sources, which is a useful property for thermal therapy applications.

Both rGO_cotton and rGO_PU2_cotton present a variable electrical response when subjected to deformation and, in particular, rGO_PU2_cotton shows a very stable signal in response to applied tensile stretching from 2.5% to 50%. rGO_PU2_cotton shows high sensitivity at lower deformations, with gauge factor values showing a precise exponential correlation to the applied deformation in all the investigated range. rGO_PU2_cotton is sensitive to the presence of humidity, showing an increased conductivity in *wet* conditions, but showing a steady piezoresistive response to stretch/release cycles, appropriate to obtain a reliable response of the sensor. Tested at 100 mm/min strain rate, rGO_PU2_cotton exhibits fast response to deformation, with response and recovery times of 500 ms and 330 ms, respectively. The durability up to 1000 deformation cycles at 100 mm/min strain rate was demonstrate by cyclic strain/release tests which showed limited hysteresis.

Finally, in comparison to other treatments reported in literature, the developed coatings induce a negligible effect on the hand of the fabrics, with flexibility and wearability comparable to pristine cotton. Therefore, the overall results demonstrate that the developed rGO/PU coatings represent very promising wash-durable coatings for the realization of electrically conductive smart fabrics and e-textiles with improved comfort and enhanced thermal conductivity for possible thermal therapy applications, and piezoresistive properties for sensing applications, such as human motion monitoring.

Author contributions The manuscript was written through the contributions of all authors. All authors have given approval to the final version of the manuscript. Conceptulization: F.O., R.C., M.L, G.G.; Data curation: F.O., F.D.F., R.C., G.G.; Funding acquisition: M.L., G.G.; Investigation: F.O., G.R., F.D.F., I.B., R.C.; Methodology: F.O., G.R., R.A., I. B., R.C., C.C., M.E.E., M.L., G.G.; Project administration: M.L., G.G.; Resources: R.A., C.C., M.E.E., G.G.; Supervision: R.C., G.G; Validation: F.O.; Visualization: F.O., R.C., M.L., G.G.; Writing – original draft: F.O., F.D.F., R.C.; Writing – review & editing: All authors.

Funding Open access funding provided by Consiglio Nazionale Delle Ricerche (CNR) within the CRUI-CARE Agreement. This work has been supported by the Italian Ministry of University and Research of Italy (MIUR) under grant PNR 2015-2020 code ARS01_00996 "TEX-STYLE - New smart and sustainable multi-sectorial textiles for creative design and Made in Italy style".

Declarations

Conflict of interest The authors declare that they have no conflict of interest.

Ethical approval The authors certify that this manuscript is original and has not been published and will not be submitted elsewhere for publication while being considered by Cellulose, and the study is not split up into several parts to increase the quantity of submissions and submitted to various journals or to one journal over time. No data have been fabricated or manipulated (including images) to support our conclusions. No data, text, or theories by others are presented as if they were our own. The submission has been received explicitly from all co-authors and authors whose names appear on the submission have contributed sufficiently to the scientific work and therefore share collective responsibility and accountability for the results.

References

Afroj S, Tan S, Abdelkader AM et al (2020) Highly conductive, scalable, and machine washable graphene-based E-textiles for multifunctional wearable electronic applications. Adv

Funct Mater 30:2000293. https://doi.org/10.1002/adfm.202000293
Bao L, Li X (2012) Towards textile energy storage from cotton T-shirts. Adv Mater 24:3246–3252. https://doi.org/10.1002/adma.201200246
Biccai S, Boland CS, Odriscoll DP et al (2019) Negative gauge factor piezoresistive composites based on polymers filled with MoS2 nanosheets. ACS Nano 13:6845–6855. https://doi.org/10.1021/acsnano.9b01613
Castaldo R, Lama GC, Aprea P et al (2019) Humidity-driven mechanical and electrical response of graphene/cloisite hybrid films. Adv Funct Mater 29:1807744. https://doi.org/10.1002/adfm.201807744
Castaldo R, Avolio R, Cocca M et al (2021) Hierarchically porous hydrogels and aerogels based on reduced graphene oxide, montmorillonite and hyper-crosslinked resins for water and air remediation. Chem Eng J. https://doi.org/10.1016/j.cej.2021.133162
Chen F, Liu H, Xu M et al (2021) Flexible cotton fabric with stable conductive coatings for piezoresistive sensors. Cellulose 28:10025–10038. https://doi.org/10.1007/s10570-021-04171-4
Chung C, Lee M, Choe EK (2004) Characterization of cotton fabric scouring by FT-IR ATR spectroscopy. Carbohydr Polym 58:417–420. https://doi.org/10.1016/j.carbpol.2004.08.005
Dall'AcquaToninVaresano LCA et al (2006) Vapour phase polymerisation of pyrrole on cellulose-based textile substrates. Synth Met 156:379–386. https://doi.org/10.1016/j.synthmet.2005.12.021
De Falco F, Gentile G, Avolio R et al (2018) Pectin based finishing to mitigate the impact of microplastics released by polyamide fabrics. Carbohydr Polym 198:175–180. https://doi.org/10.1016/j.carbpol.2018.06.062
De Falco F, Cocca M, Guarino V et al (2019a) Novel finishing treatments of polyamide fabrics by electrofluidodynamic process to reduce microplastic release during washings. Polym Degrad Stab 165:110–116. https://doi.org/10.1016/j.polymdegradstab.2019.05.001
De Falco F, Guarino V, Gentile G et al (2019b) Design of functional textile coatings via non-conventional electrofluidodynamic processes. J Colloid Interface Sci 541:367–375. https://doi.org/10.1016/j.jcis.2019.01.086
Ergoktas MS, Bakan G, Steiner P et al (2020) Graphene-enabled adaptive infrared textiles. Nano Lett 20:5346–5352. https://doi.org/10.1021/acs.nanolett.0c01694
Eskandarian L, Lam E, Rupnow C et al (2020) Robust and multifunctional conductive yarns for biomedical textile computing. ACS Appl Electron Mater 2:1554–1566. https://doi.org/10.1021/acsaelm.0c00171
Gao W, Alemany LB, Ci L, Ajayan PM (2009) New insights into the structure and reduction of graphite oxide. Nat Chem 1:403–408. https://doi.org/10.1038/nchem.281
Ghosh S, Ghosh R, Guha PK, Bhattacharyya TK (2015) Humidity sensor based on high proton conductivity of graphene oxide. IEEE Trans Nanotechnol 14:931–937. https://doi.org/10.1109/TNANO.2015.2465859
Hong X, Yu R, Hou M et al (2021) Smart fabric strain sensor comprising reduced graphene oxide with structure-based negative piezoresistivity. J Mater Sci 56:16946–16962. https://doi.org/10.1007/s10853-021-06365-4
Hwang HJ, Yeon JS, Jung Y et al (2021) Extremely foldable and highly porous reduced graphene oxide films for shape-adaptive triboelectric nanogenerators. Small 17:1903089. https://doi.org/10.1002/smll.201903089
Irimia-Vladu M, Głowacki ED, Voss G et al (2012) Green and biodegradable electronics. Mater Today 15:340–346. https://doi.org/10.1016/S1369-7021(12)70139-6
Jiang X, Ren Z, Fu Y et al (2019) Highly compressible and sensitive pressure sensor under large strain based on 3D porous reduced graphene oxide fiber fabrics in wide compression strains. ACS Appl Mater Interfaces 11:37051–37059. https://doi.org/10.1021/acsami.9b11596
Karim N, Afroj S, Tan S et al (2017) Scalable production of graphene-based wearable E-textiles. ACS Nano 11:12266–12275. https://doi.org/10.1021/acsnano.7b05921
Karim N, Afroj S, Tan S et al (2019) All inkjet-printed graphene-silver composite ink on textiles for highly conductive wearable electronics applications. Sci Rep 9:1–10. https://doi.org/10.1038/s41598-019-44420-y
Kim SJ, Song W, Yi Y et al (2018) High durability and waterproofing rGO/SWCNT-fabric-based multifunctional sensors for human-motion detection. ACS Appl Mater Interfaces 10:3921–3928. https://doi.org/10.1021/acsami.7b15386
Ko J, Jee S, Lee JH, Kim SH (2018) High durability conductive textile using MWCNT for motion sensing. Sensors Actuators, A Phys 274:50–56. https://doi.org/10.1016/j.sna.2018.02.037
Li H, Zhang W, Ding Q et al (2019) Facile strategy for fabrication of flexible, breathable, and washable piezoelectric sensors via welding of nanofibers with multiwalled carbon nanotubes (MWCNTs). ACS Appl Mater Interfaces 11:38023–38030. https://doi.org/10.1021/acsami.9b10886
Li Y, Miao X, Chen JY et al (2021) Sensing performance of knitted strain sensor on two-dimensional and three-dimensional surfaces. Mater Des 197:109273. https://doi.org/10.1016/j.matdes.2020.109273
Nair RR, Wu HA, Jayaram PN et al (2012) Unimpeded permeation of water through helium-leak–tight graphene-based membranes. Science 335:442–444. https://doi.org/10.1126/science.1211694
Oh KW, Hong KH, Kim SH (1999) Electrically conductive textiles by in situ polymerization of aniline. J Appl Polym Sci 74:2094–2101. https://doi.org/10.1002/(SICI)1097-4628(19991121)74:8%3c2094::AID-APP26%3e3.0.CO;2-9
Park S, An J, Potts JR et al (2011) Hydrazine-reduction of graphite- and graphene oxide. Carbon N Y 49:3019–3023. https://doi.org/10.1016/j.carbon.2011.02.071
Parnell S, Min K, Cakmak M (2003) Kinetic studies of polyurethane polymerization with Raman spectroscopy. Polymer 44:5137–5144. https://doi.org/10.1016/S0032-3861(03)00468-3
Pei S, Cheng HM (2012) The reduction of graphene oxide. Carbon N Y 50:3210–3228. https://doi.org/10.1016/j.carbon.2011.11.010
Ren J, Wang C, Zhang X et al (2017) Environmentally-friendly conductive cotton fabric as flexible strain sensor based on

hot press reduced graphene oxide. Carbon 111:622–630. https://doi.org/10.1016/j.carbon.2016.10.045
Repon MR, Mikučionienė D (2021) Progress in flexible electronic textile for heating application: A critical review. Materials 14:6540–6564. https://doi.org/10.3390/ma14216540
Roeges NPG (1994) A guide to the complete interpretation of infrared spectra of organic structures. Wiley, New York
Rollo G, Zullo R, Bonadies I et al (2022) Synergistic effect of phase change materials and reduced graphene oxide in enhancing the thermoregulating properties of polymeric composites. J Mater Sci. https://doi.org/10.1007/s10853-022-08045-3
Roohpour N, Wasikiewicz JM, Moshaverinia A et al (2009) Isopropyl myristate-modified polyether-urethane coatings as protective barriers for implantable medical devices. Materials 2:719–733. https://doi.org/10.3390/ma2030719
Sahito IA, Sun KC, Arbab AA et al (2015) Graphene coated cotton fabric as textile structured counter electrode for DSSC. Electrochim Acta 173:164–171. https://doi.org/10.1016/j.electacta.2015.05.035
Shateri-Khalilabad M, Yazdanshenas ME (2013) Fabricating electroconductive cotton textiles using graphene. Carbohydr Polym 96:190–195. https://doi.org/10.1016/j.carbpol.2013.03.052
Shathi MA, Chen M, Khoso NA et al (2020) Graphene coated textile based highly flexible and washable sports bra for human health monitoring. Mater Des 193:108792. https://doi.org/10.1016/j.matdes.2020.108792
Shi HF, Wang C, Sun ZP et al (2015) Transparent conductive reduced graphene oxide thin films produced by spray coating. Sci China Physics, Mech Astron 58:1–5. https://doi.org/10.1007/s11433-014-5614-y
Souri H, Bhattacharyya D (2018) Highly stretchable multifunctional wearable devices based on conductive cotton and wool fabrics. ACS Appl Mater Interfaces 10:20845–20853. https://doi.org/10.1021/acsami.8b04775
Souri H, Bhattacharyya D (2022) Wool fabrics decorated with carbon-based conductive ink for low-voltage heaters. Mater Adv 3:3952–3960. https://doi.org/10.1039/D1MA00981H
Stanković SB, Popović D, Poparić GB (2008) Thermal properties of textile fabrics made of natural and regenerated cellulose fibers. Polym Test 27:41–48. https://doi.org/10.1016/j.polymertesting.2007.08.003
Trovati G, Sanches EA, Neto SC et al (2010) Characterization of polyurethane resins by FTIR, TGA, and XRD. J Appl Polym Sci 115:263–268. https://doi.org/10.1002/APP.31096
Tuinstra F, Koenig JL (2003) Raman spectrum of graphite. J Chem Phys 53:1126. https://doi.org/10.1063/1.1674108
Wang B, Facchetti A (2019) Mechanically flexible conductors for stretchable and wearable E-skin and E-textile devices. Adv Mater 31:1–53. https://doi.org/10.1002/adma.201901408
Wang Y, Wang W, Xu R et al (2019) Flexible, durable and thermal conducting thiol-modified rGO-WPU/cotton fabric for robust electromagnetic interference shielding. Chem Eng J 360:817–828. https://doi.org/10.1016/j.cej.2018.12.045
Yaghoubidoust F, Salimi E (2019) A simple method for the preparation of antibacterial cotton fabrics by coating graphene oxide nanosheets. Fibers Polym 20:1155–1160. https://doi.org/10.1007/s12221-019-8540-1
Yao Y, Chen X, Zhu J et al (2012) The effect of ambient humidity on the electrical properties of graphene oxide films. Nanoscale Res Lett 7:2–19. https://doi.org/10.1186/1556-276X-7-363
Yetisen AK, Qu H, Manbachi A et al (2016) Nanotechnology in textiles. ACS Nano 10:3042–3068. https://doi.org/10.1021/acsnano.5b08176
Yu Q, Weng P, Han L et al (2019) Enhanced thermal conductivity of flexible cotton fabrics coated with reactive MWCNT nanofluid for potential application in thermal conductivity coatings and fire warning. Cellulose 26:7523–7535. https://doi.org/10.1007/s10570-019-02592-w
Zhang X, Chao X, Lou L et al (2021) Personal thermal management by thermally conductive composites: A review. Compos Commun 23:100595. https://doi.org/10.1016/j.coco.2020.100595
Zhao Y, Wang J, Li Z et al (2020) Washable, durable and flame retardant conductive textiles based on reduced graphene oxide modification. Cellulose 27:1763–1771. https://doi.org/10.1007/s10570-019-02884-1
Zheng Y, Liu H, Chen X et al (2022) Wearable thermoelectric-powered textile-based temperature and pressure dual-mode sensor arrays. Org Electron 106:106535. https://doi.org/10.1016/j.orgel.2022.106535
Zhou G, Byun J-H, Oh Y et al (2017) Highly sensitive wearable textile-based humidity sensor made of high-strength, single-walled carbon nanotube/poly (vinyl alcohol) filaments. ACS Appl Mater Interfaces 9:4788–4797. https://doi.org/10.1021/acsami.6b12448
Zhu S, Wang M, Qiang Z et al (2021) Multi-functional and highly conductive textiles with ultra-high durability through 'green' fabrication process. Chem Eng J 406:127140. https://doi.org/10.1016/j.cej.2020.127140